Dendrochronologia 66 (2021) 125812

Contents lists available at ScienceDirect

Dendrochronologia

journal homepage: www.elsevier.com/locate/dendro

ORIGINAL ARTICLE

Drought and cold spells trigger dieback of temperate oak and beech forests in northern Spain

J. Julio Camarero [a,*], Michele Colangelo [a,b], Antonio Gazol [a], Cesar Azorín-Molina [c]

[a] Instituto Pirenaico De Ecología, Consejo Superior De Investigaciones Científicas (IPE-CSIC), Avda. Montañana 1005, Apdo. 202, 50192 Zaragoza, Spain
[b] School of Agricultural, Forest, Food and Environmental Sciences, Univ. Basilicata, Potenza, I-85100, Italy
[c] Centro De Investigaciones Sobre Desertificación, Consejo Superior De Investigaciones Científicas (CIDE-CSIC), Montcada, Valencia, Spain

ARTICLE INFO

Keywords:
Dendroecology
Early-warning signals
Fagus sylvatica
Quercus humilis
Quercus robur
Water-use efficiency

ABSTRACT

Dieback in temperate forests is understudied, despite this biome is predicted to be increasingly affected by more extreme climate events in a warmer world. To evaluate the potential drivers of dieback we reconstructed changes in radial growth and intrinsic water-use efficiency (iWUE) from stable isotopes in tree rings. Particularly, we compared tree size, radial-growth trends, growth responses to climate (temperature, precipitation, cloudiness, number of foggy days) and drought, and changes in iWUE of declining and non-declining trees showing contrasting canopy dieback and defoliation. This comparison was done in six temperate forests located in northern Spain and based on three broadleaved tree species (*Quercus robur*, *Quercus humilis*, *Fagus sylvatica*). Declining trees presented lower radial-growth rates than their non-declining counterparts and tended to show lower growth variability, but not in all sites. The growth divergence between declining and non-declining trees was significant and lasted more in *Q. robur* (15–30 years) than in *F. sylvatica* (5–10 years) sites. Dieback was linked to summer drought and associated atmospheric patterns, but in the wettest *Q. robur* sites cold spells contributed to the growth decline. In contrast, *F. sylvatica* was the species most responsive to summer drought in terms of growth reduction followed by *Q. humilis* which showed coupled changes in growth and iWUE as a function of tree vigour. Low growth rates and higher iWUE characterized declining *Q. robur* and *F. sylvatica* trees. However, declining *F. sylvatica* trees became less water-use efficient close to the dieback onset, which could indicate impending tree death. In temperate forests, dieback and growth decline can be triggered by climate extremes such as dry and cold spells, and amplified by climate warming and rising drought stress.

1. Introduction

Climate warming is making temperate forests to be more limited by water availability (Babst et al., 2019). These forests are often dominated by broadleaf hardwood species or by conifers, and subjected to seasonal cool and wet conditions, but they are also vulnerable to acute heat- and drought-stress (Allen et al., 2015). In this biome, water shortage and heat waves have already caused reductions in forest productivity, decreased carbon uptake and nutrient assimilation, altered carbon allocation and enhanced water-use efficiency (Bréda et al., 2006, Camarero and Fajardo, 2017, D'Orangeville et al., 2018; Rubio-Cuadrado et al., 2018). Drought and reduced soil moisture also diminished leaf area of affected tree species, either through early senescence or partial canopy dieback, reducing carbohydrate pools and radial growth (Fritts, 1962; Filewod and Thomas, 2014). For instance, droughts have synchronized abrupt growth declines across north-eastern America (Pederson et al., 2014) and central Europe temperate forests (Zang et al., 2014) conditioning post-drought recovery (Druckenbrod et al., 2019).

The tolerance to drought, in terms of growth recovery or loss, varies among tree species and populations of temperate forests. In the case of shade-tolerant angiosperms, such as oak and beech, they tend to present a high growth resistance but a low resilience (Zang et al., 2014; Gazol et al., 2017,). Different drought responses have been also documented in mixed oak-beech stands with better performance for beech (Pretzsch et al., 2013). However, we lack long-term assessments of the responses of oak and beech forests to droughts causing dieback (*sensu* Manion, 1981). This information is urgently needed to forecast how warmer and drier conditions will affect the vitality of temperate forests and under which conditions dieback will occur.

Severe drought can impair the hydraulic functioning and carbon

* Corresponding author.
E-mail address: jjcamarero@ipe.csic.es (J.J. Camarero).

https://doi.org/10.1016/j.dendro.2021.125812
Received 20 September 2020; Received in revised form 5 January 2021; Accepted 15 January 2021
Available online 20 January 2021

balance of broadleaves leading to dieback and tree death (Adams et al., 2017). Global comparisons of conspecific surviving and dying trees found strong and long-lasting declines in radial growth before tree death in gymnosperms, but shade-tolerant angiosperms tended to show small and short-term (median 16 years) growth reductions preceding tree death (Cailleret et al., 2017). In that analysis, oaks showed fast growth declines before tree death (see also Pedersen, 1998), which agrees with its low resilience and short-term post-drought legacies (Anderegg et al., 2015). However, gymnosperms are much more represented than angiosperms in global assessments of growth patterns (Cailleret et al., 2017) and physiological mechanisms (Adams et al., 2017) of drought-induced dieback and tree mortality. Here we aim at filling that research gap by complementing tree-ring data with physiological information derived from carbon isotope data measured in wood. We also analyze if growth and isotope patterns can be complemented and used as early-warning signals (cf. Camarero et al., 2015) of tree death since current algorithms based solely on growth data have poor predictive power in some broadleaf species (Pedersen, 1998; Wyckoff and Clark, 2002).

The equatorward limit (rear edge) of temperate forests is formed by either subtropical or Mediterranean biomes and forests near that limit face variable dry conditions (Frelich et al., 2015). This is the case of northern Spain, where major European hardwood species find their southernmost distribution limits such as the pedunculate oak (*Quercus robur* L.) and the European beech (*Fagus sylvatica* L.), but also sub-Mediterranean, transitional species as the downy oak (*Quercus humilis* Mill.). These rear-edge populations are occurring at sites with suboptimal conditions in temperate areas with variable Mediterranean influence, characterized by warm and dry conditions during the growing season (Giorgi and Lionello, 2008). It could be expected that forecasted hotter droughts (droughts accompanied by warmer temperatures) will reduce growth of these marginal tree populations, and trigger forest dieback rising mortality rates (Sánchez-Salguero et al., 2017). Since the regional thermal and rainfall regimes in Mediterranean areas, and therefore forest growth, depend on atmospheric patterns such as the Northern Atlantic Oscillation (NAO) (Camarero, 2011), we also explored their links with tree growth. In this study, we followed a multi-proxy approach (Colangelo et al., 2017a), and analysed the radial-growth patterns and carbon isotope discrimination of coexisting, conspecific trees showing different canopy dieback (declining vs. non-declining trees) of three broadleaf species (*Q. robur*, *Q. humilis* and *F. sylvatica*). We also modelled growth trends, analysed early-warning growth signals and quantified the growth responses to climate variables and drought. By analyzing the $\delta^{13}C$ of wood the intrinsic water-use efficiency (iWUE), which is the ratio between photosynthesis (A) and stomatal conductance (g_s) rates, was calculated to reconstruct water- and gas-exchange dynamics (Farquhar et al., 1982, 1989).

In comparison with non-declining trees, we hypothesize that declining trees will show: (i) lower radial-growth rates and variability in response to drought, (ii) higher growth responsiveness to warmer and drier conditions during the growing season, and (iii) a poorer ability to regulate gas exchange and water loss through leaves, i.e. a lower iWUE due to low A and/or high g_s (cf. Hentschel et al., 2016). Following Gessler et al. (2018) we also expect that declining trees will show a sudden growth drop and be water-use inefficient. Alternatively, lower growth but higher iWUE might be a consequence of increased transpiration rates and reduced g_s, a plausible scenario in the moderately anisohydric *F. sylvatica* (cf. Pflug et al., 2018) than in anisohydric oaks. We also expect that tree death can be preceded by a tipping point in radial growth, representing a critical transition from non-declining to declining growth patterns.

2. Materials and methods

2.1. Study sites and tree species

We studied two stands per species showing recent climate-related dieback according to local forest managers and owners, who checked for the lack of influence of pathogens and pests on tree vigour. In the selected stands, the spatial pattern of dieback was characterized by patchy or scattered groups of declining and recently dead trees affecting at least 25 % of the individuals. Study sites are located in northern Spain (see their characteristics in Table 1 and Fig. S1). The study forests are pure, uneven aged stands resulting from sexual reproduction and not subjected to silvicultural treatments as thinning or coppicing at least since the 1960s.

In the case of *Q. robur*, we selected two rather flat sites with high forests and deep, well-developed, clay soils (Beluntza and Alsasua) presenting dominant trees with abundant crown dieback across approx. 10 ha (Fig. S1). In these sites, soils can be waterlogged in winter and dry in summer. Other woody plant species present in these forests are: *Corylus avellana, Crataegus monogyna, Ilex aquifolium*, and *Hedera helix*. The basal area ranges between 20 and 40 $m^2\ ha^{-1}$ and the density between 400 and 600 stem ha^{-1}.

The two *Q. humilis* stands were high forests (Galdeano and Aramendia, Table 1), with basic soils and understory dominated by *Buxus sempervirens*, *Juniperus oxycedrus* and *Crataegus monogyna*. In these sites, tree density was similar (1150 stem ha^{-1}), but basal area was higher in Galdeano (66.2 $m^2\ ha^{-1}$), where oak coexisted with *F. sylvatica*, than in Aramendia (36.9 $m^2\ ha^{-1}$), where oak coexisted with the drought-tolerant Holm oak (*Quercus ilex*), and dieback was more intense according to defoliation and growth data (see Table 2).

In the *F. sylvatica* sites (Eraso and Lokiz, Table 1), the understory includes *Juniperus communis*, *Prunus spinosa* and *Rosa canina*, and soils are thin and developed on limestones. The basal area was higher in Lokiz (29.0 $m^2\ ha^{-1}$) than in Eraso (24.5 $m^2\ ha^{-1}$). The two sites are high forests, i.e. stands mainly regenerated from seedlings with long rotation periods, but open areas were also found in Lokiz corresponding to past thinning in the 1950s (Fig. S1).

In the northernmost sites (Beluntza, Alsasua and Eraso), climatic conditions are mild and temperate according to local data with mean annual air temperature of 11.4 °C and annual precipitation ranging between 793 and 1208 mm. However, in the southern sites (Galdeano, Aramendia, Lokiz) climate conditions are drier with mean annual temperature of 12.6 °C and annual precipitation ranging between 620 and 845 mm. The driest and warmest months are July and August, whereas the wettest period is from November to January and the coldest months are January and February. Frosts occur during winter. The climatic water balance is negative from June to September in southern sites.

The three study species are winter deciduous. Oaks form ring-porous wood, but beech forms diffuse-porous wood. *F. sylvatica* is a late-successional which outcompetes oak when they coexist in the beech optimum (Cavin et al., 2013). Both oak species are shade-intolerant with *Q. robur* dominant in valley bottoms with high potential soil water availability, and *Q. humilis* found in mountain sites with low different potential soil water availability across central and southern Europe (Damesin and Rambal, 1995). Since the two study oaks hybridize, we selected pure stands and checked morphological features (leaf and fruit shape, bark) to distinguish each species (Granda et al., 2017).

2.2. Field sampling

The two sites selected for each species showed clear symptoms of drought-triggered dieback, including abundant trees showing crown dieback, growth alterations (e.g., abundant epicormic shoots and dead buds and branches) and severe growth reduction or tree death after recent dry or warm spells (Table 1, Fig. S1). We sampled pairs of dominant trees showing contrasting crown transparency or defoliation,

Table 1
Sites dominated by temperate hardwood species (oaks, European beech) showing recent dieback episodes in northern Spain.

Tree species	Site (code)	Latitude (N)	Longitude (W)	Elevation (m a.s.l.)	Slope (°)	Orientation	Year of dieback onset	Timespan of tree-ring width series
Quercus robur	Beluntza (BE)	42° 57′ 06″	2° 53′ 25″	610	2°	S	2017	1824–2017
	Alsasua (AL)	42° 53′ 50″	2° 05′ 03″	615	5°	N-NE	2016	1851–2017
Quercus humilis	Galdeano (GA)	42° 44′ 06″	2° 06′ 26″	649	22°	S	2017	1937–2017
	Aramendia (AR)	42° 42′ 59″	2° 06′ 42″	683	5°	SE	2017	1925–2017
Fagus sylvatica	Eraso (ER)	42° 57′ 10″	1° 48′ 02″	547	10º	W	2017	1890–2016
	Lokiz (LO)	42° 43′ 16″	2° 10′ 36″	1010	15°	N-NE	2016	1768–2017

Table 2
Size and growth variables of the sampled trees. Tree type: ND, non-declining tree, D, declining tree. Different letters indicate significant ($p < 0.05$) differences according to *t* tests.

Species	Site	Tree type	Defoliation (%)	Dbh (cm)	Height (m)	Age (yrs.)	No trees	Mean tree-ring width (mm)	Correlation with mean series
Q. robur	BE	ND	5 ± 1a	53.7 ± 1.1b	27.1 ± 0.6b	145 ± 27	18	1.30 ± 0.05b	0.58 ± 0.02b
		D	85 ± 5b	45.3 ± 1.1a	23.8 ± 0.5a	148 ± 22	15	1.01 ± 0.06a	0.47 ± 0.02a
	AL	ND	6 ± 1a	46.9 ± 2.5	15.8 ± 0.3b	112 ± 6	15	1.75 ± 0.15b	0.45 ± 0.03
		D	82 ± 3b	44.7 ± 2.4	14.6 ± 0.4a	125 ± 3	12	1.20 ± 0.09a	0.46 ± 0.01
Q. humilis	GA	ND	15 ± 2a	29.1 ± 0.6	16.6 ± 0.3	61 ± 2	10	1.83 ± 0.08b	0.52 ± 0.03
		D	60 ± 3b	28.8 ± 1.8	16.3 ± 0.7	59 ± 3	10	1.54 ± 0.06a	0.49 ± 0.04
	AR	ND	5 ± 1a	27.1 ± 0.7b	11.4 ± 0.2b	69 ± 9	17	1.29 ± 0.08b	0.61 ± 0.03b
		D	80 ± 2b	21.7 ± 0.7a	9.2 ± 0.5a	74 ± 10	15	0.90 ± 0.04a	0.42 ± 0.03a
F. sylvatica	ER	ND	6 ± 1a	32.2 ± 2.9	14.1 ± 0.1	88 ± 9	10	1.95 ± 0.14b	0.41 ± 0.01
		D	64 ± 6b	34.6 ± 3.3	14.0 ± 0.1	93 ± 8	10	1.38 ± 0.04a	0.39 ± 0.01
	LO	ND	7 ± 2a	47.3 ± 4.4	15.3 ± 0.5b	148 ± 55	20	1.32 ± 0.11b	0.49 ± 0.03
		D	83 ± 3b	40.3 ± 3.8	13.8 ± 0.6a	142 ± 55	23	1.08 ± 0.06a	0.45 ± 0.03

here considered a proxy of tree vigour (Dobbertin, 2005). Sampled neighbouring trees were always located approx. 10−15 m from each other. For each tree, we measured its diameter at breast height (Dbh, at 1.3 m) and total stem height using tapes and a Nikon Forestry 550 rangefinder (Nikon Inc., Tokyo), respectively. We obtained two defoliation percentages per tree taken by different observers (visual assessments) and calculated its average. Declining and non-declining trees were considered those having crown defoliation ≥ 60 % and < 60 %, respectively. This threshold is similar to the canopy dieback (58 %) which allows differentiating dead and surviving *F. sylvatica* trees (Chakraborty et al., 2017).

2.3. Climate data, drought and climate indices

To obtain long-term climate data (monthly mean maximum and minimum air temperature, total precipitation and cloud cover) we used the E-OBS v. 17.0 0.1°-gridded dataset considering the 1950 − 2016 period (Moreno and Hasenauer, 2015; Cornes et al., 2018). For cloud cover data, we used the CRU TS v. 4.02 0.5°-gridded dataset (Harris et al., 2014). We downloaded these data for the grids including each site using the Climate Explorer webpage (https://climexp.knmi.nl).

The monthly number of foggy days was obtained from local observations taken in nearby stations of the Spanish Meteorological Agency (AEMET) network for the 1960 − 2016 period. A foggy day is registered by AEMET weather observers when the suspension in the air of very small drops of water reduces horizontal visibility to less than 1 km. A fog bank can occupy large flat areas, or appear in the form of scattered banks of small extension (up to a few square kilometers). Fogs can dissipate in few hours, usually after sunrise, or remain for periods of up to a day or more. Specifically, we processed and obtained these data for the following stations: Foronda-Txokiza (42.90 °N, 2.18 °W, 523 m a.s.l., located at 14 km from Beluntza site), Alsasua (42.88 °N, 2.73 °W, 513 m a.s.l., located at 6 and 30 km from Alsasua and Eraso sites, respectively), and Estella (42.66 °N, 2.04 °W, 437 m a.s.l., located at 7, 8 and 10 km from Galdeano, Aramendia and Lokiz sites). In the study sites, the monthly number of foggy days ranges from 3 to 6 from September to January with maximum and minimum values in the Foronda-Txokiza and Estella stations, respectively.

To assess drought severity, we obtained weekly values of the Standardized Precipitation Evapotranspiration Index (SPEI) for the same 0.1° grids as above and for 1962–2016. We obtained SPEI data at 1-, 3-, 6-, and 9-month resolutions (Vicente-Serrano et al., 2017). The SPEI is a drought index which accounts for temporal differences in drought severity with negative and positive values corresponding to dry and moist conditions, respectively (Vicente-Serrano et al., 2010). For the growth models, we selected 3-month July SPEI following Pasho et al. (2011).

Since previous findings showed that the regional rainfall regime and forest growth in northern Spain depend on several atmospheric patterns and teleconnections (Rozas et al., 2015), we also explored their links with tree growth. This analysis could reveal if forest dieback is related to changing regional atmospheric and climatic patterns (cf. Camarero, 2011). We considered the NAO which determines winter precipitation and air temperature over northern Spain (Camarero, 2011). Positive and negative NAO phases correspond to dry-warm and cool-wet winter--spring conditions, respectively. We also included the Southern Oscillation Index (SOI) which accounts for the influences of El Niño-Southern Oscillation (ENSO) on Iberian rainfall patterns (Rodó et al., 1997). In Iberia, positive correlations between SOI and spring rainfall were found by Rodó et al. (1997). Finally, we considered the Western Mediterranean Oscillation index (WeMO) which captures rainfall patterns, mainly from autumn to winter, over northern and eastern Iberian Peninsula (Martín-Vide and López-Bustins, 2006). The WeMO is measured as the difference in pressure between northern Italy (Padua) and south west Spain (Cádiz) and reflects the synoptic variability of the western Mediterranean Basin. Positive WeMO phases correspond to high pressures over Iberia and low precipitation amounts, and negative WeMO phases correspond to rainy conditions over Spain, especially during autumn. Climate indices were downloaded from the CRU (NAO and SOI, https://crudat a.uea.ac.uk/cru/data) and from the Climatology Group of University of Barcelona websites (WeMO, http://www.ub.edu/gc/wemo/).

2.4. Tree-ring data

In each site, we cored 12–15 declining or very defoliated trees and 12–15 non-declining or less defoliated trees at 1.3 m using Pressler increment borers. We took two cores per tree in opposite directions and always perpendicular to the slope. Cores were air dried, sanded, and visually cross-dated. Then, we used a binocular scope and a LINTAB measuring device (Rinntech, Germany) to measure the tree-ring widths to the nearest 0.01 mm. The accuracy of visual cross-dating was checked using the COFECHA software which calculates moving correlations between each individual series and the mean site series (Holmes, 1983).

The ring-width series were standardized and detrended by fitting 40-year cubic smoothing splines with a 50 % cut-off frequency to remove age- and size-related long- to mid-frequency growth variability. Then, the resulting individual series of ring-width indices were pre-whitened with autoregressive (AR) models, and averaged for each vigour class and site by using bi-weight robust means. The order of the AR models was selected by minimizing the Akaike Information Criterion (Akaike, 1974). The detrending procedures were done using the software ARSTAN ver.44 (Cook and Krusic, 2005).

We checked the normality of the series of ring-width indices using the Shapiro–Wilk test. We used Pearson and Spearman correlations to quantify the statistical relationship (at the $p < 0.05$ level) between mean series of pre-whitened ring-width indices and climate variables following (mean maximum and minimum air temperatures, precipitation, NAO, SOI and WeMO) or not following (number of foggy days) normal distributions, respectively. Correlations were calculated from the previous to the current September. To assess how climate-growth correlations changed through time, we also calculated moving correlations calculated between climate variables, selected in previous correlation analyes, and mean series of ring-width indices of declining and non-declining trees considering 20-year long intervals.

2.5. Modeling tree growth in declining and non-declining trees

All statistical analyses were performed using the R software v. 3.6.2 (R Development Core Team, 2019). We modelled radial growth (raw ring-width data) of declining and non-declining trees using generalized additive mixed models (GAMMs, Wood, 2006). A similar approach was followed by Camarero et al. (2015). We considered as predictor variables: tree size (Dbh), vigour class and interactions with calendar year. Separate analyses were performed for each site since we assumed different growth trends for declining and non-declining trees in each site. Tree identity was included as a random factor to account for the fact that growth data are repeated measures over an individual. Growth trends were modelled using a thin plate regression spline with a maximum number of six degrees of freedom. Calendar year was considered an explanatory variable. To account for growth divergences between declining and non-declining trees we also considered interactions between calendar year and vigour class. To consider ontogenetic changes in tree size, Dbh was included as a fixed factor. Tree-ring width was log-transformed (log(x+1)) prior to the analyses to achieve normality. We included a first-order autocorrelation structure (AR1) to account for dependency of growth in year t on the growth of the previous year $t-1$.

$$Log\left(TRW_{ij}+1\right) = f_1(DHB_i) + f_2\left(year_j,\ vigour_i\right) + AR1 + Z_{ij} \quad (1)$$

where TRW_{ij} is the tree-ring width of the tree i in the year j, DBH_i, $vigour_i$ are the diameter at breast height and vigour of the tree i, year is the calendar year, AR1 is the growth autocorrelation, and Z_{ij} is the matrix of random effects.

2.6. Early-warning growth signals and other statistical analyses

We applied different statistics to detect early-warning signals of critical transitions in tree growth (Dakos et al., 2012). Particularly, we studied whether the tree-ring width of each species for the period 1950–2016 showed changes in standard deviation (SD). To this end, we estimated the values in SD within 20-year rolling windows along the period 1950–2016. Separate analyses were performed for declining and non-declining individuals of each species. Prior to the analyses, individual measures of tree-ring width were averaged using a bi-weight robust mean. The R Early Warning Signals toolbox was used to calculate the SD series (Dakos et al., 2012).

Comparisons between declining and non-declining trees were carried out using t test. Trends in climate variable (for 1950–2016) and ring-width data were assessed using the Kendall τ statistic. Statistical significance for the t test and trends was measured at the $p < 0.05$ level.

2.7. Calculating intrinsic water-use efficiency

We selected one site per species (Beluntza for *Q. robur*, Aramendia for *Q. humilis*, and Lokiz for *F. sylvatica*) to calculate iWUE in declining and non-declining trees. These sites were selected because declining and non-declining trees were dominant and showed similar ages, but presented clearly diverging growth trends during the last decades. First, we pooled 5-ring samples of five declining trees and five non-declining trees in each site. We considered eight 5-ring periods (1968–1972, 1973–1977, 1978–1982, 1983–1987, 1988–1992, 1993–1997, 1998–2002, and 2003–2007). Second, we also compared individual samples of the two most recent 5-year periods (2008–2012, 2013–2017) in five declining trees and five non-declining trees of each species.

We measured carbon isotope composition ($\delta^{13}C$) in tree-ring wood to estimate iWUE, which can be defined as the ratio between the net photosynthetic rate (A) and the stomatal conductance (g_s) (Farquhar et al., 1982, 1989). Pooled and individual wood samples were homogenized to a fine powder using a ball mixer mill (Retsch MM301, Haan, Germany). Wood aliquots (0.001 g) were weighted on a microbalance (AX205 Mettler Toledo, OH, USA), stored in tin foil capsules, and combusted to CO_2 using a Flash EA-1112 elemental analyser interfaced with a Finnigan MAT Delta C isotope ratio mass spectrometer (Thermo Fisher Scientific Inc., MA, USA). Isotope analyses were performed at the Stable Isotope Facility, University of California at Davis (USA). Stable isotope ratios were expressed as deviations (‰) using the δ notation relative to the VPDB standard. The standard deviation for repeated $\delta^{13}C$ analyses was 0.06‰.

3. Results

3.1. Climate trends and extreme climate events

Temperatures have increased in all sites for 1950-2016, whereas precipitation and cloud cover have decreased in summer and September (Table S1). The number of foggy days has decreased in September in Alsasua and Eraso, in August in Beluntza and in June in the other sites. In addition, we also detected a winter cold spell which affected the Beluntza *Q. robur* site due to a drop in minimum air temperatures in January 1971 (Fig. S2). According to SPEI data, the main droughts in the study sites occurred in 1982, 1986, 1995, 2005 and 2012 (Fig. S3). They were mainly short-term droughts (1- to 3-months SPEI values from January to September).

3.2. Tree size, defoliation and growth

In all sites, declining trees showed lower radial-growth rates than non-declining trees (Figs. S4, S5 and S6). In the Beluntza *Q. robur* site and in the Aramendia *Q. humilis* site, declining trees showed a smaller Dbh than non-declining trees (Table 2). In four out of six sites, declining trees showed lower height than non-declining trees, except in the Galdeano *Q. humilis* and the Eraso *F. sylvatica* sites. Regarding the correlation of the individual ring-width series with the mean series of each site

and vigour class, declining trees showed lower correlation values than non-declining trees in the Beluntza *Q. robur* site and in the Aramendia *Q. humilis* site.

3.3. Modeled growth trends as a function of tree vigour

Growth trends of declining and non-declining trees significantly diverged in three sites for the last 10–30 years (the Beluntza and Alsasua *Q. robur* sites, and the Eraso *F. sylvatica* site, Fig. 1). The largest percentage of variation was explained in Galdeano (Table 3), where differences between declining and non-declining trees were more noticeable in the 1980s than nowadays (Fig. 1). Differences in growth trends between declining and non-declining trees were very noticeable in the last two to three decades in Beluntza, Alsasua, Eraso and Lokiz. However, the lowest percentage of explained variance (21 %) was found in *F. sylvatica* sites (i.e. Eraso and Alsasua), suggesting that growth trends vary considerably between individuals within the declining and non-declining groups in this species.

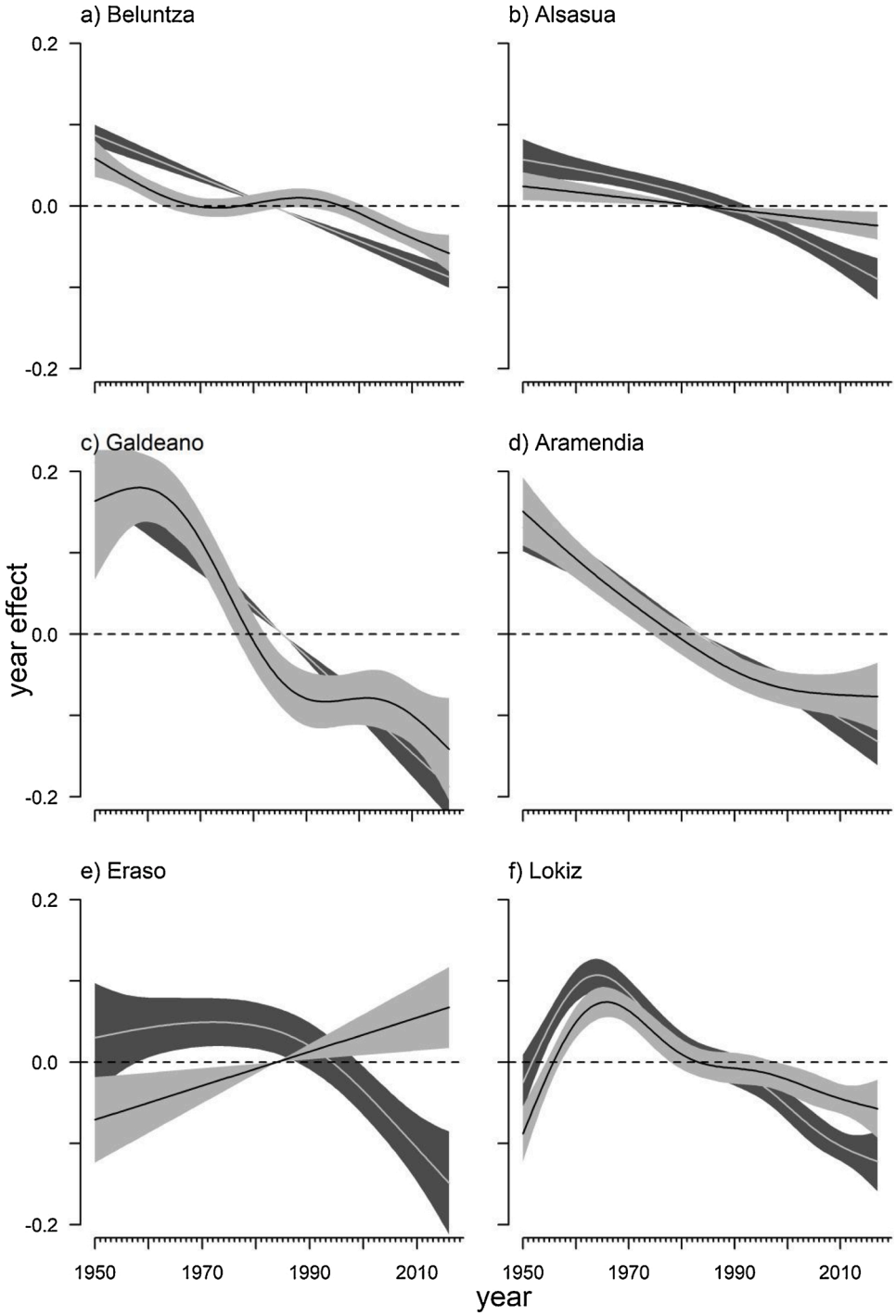

Fig. 1. Long-term growth trends (year effect) of declining (dark-grey bands) and non-declining (light grey bars) trees in each site according to GAMMs. The plots show the effects of year on tree-ring width (see Table 3). Two sites per species were considered: *Q. robur* (a, b), *Q. humilis* (c, d) and *F. sylvatica* (e, f). The line represents the effect and the shaded area the standard errors.

Table 3
Generalized additive mixed-models (GAMMs) of growth (tree-ring width) for each site and tree species. For the linear terms, the *t* statistic is shown, whereas for parameters modelled with spline functions the *F* values are shown (edf are given between parentheses). The R^2 associated with each model is presented. Variables' abbreviations: ND and D, non-declining and declining trees, respectively (vigour classes), Dbh, diameter at breast height. Significance levels: $p < 0.05$*, $p < 0.01$**.

Variables	Site (tree species)					
	Beluntza (*Q. robur*)	Alsasua (*Q. robur*)	Galdeano (*Q. humilis*)	Aramendia (*Q. humilis*)	Eraso (*F. sylvatica*)	Lokiz (*F. sylvatica*)
Linear terms						
Vigour (ND)	5.33**	4.79**	1.49	3.87**	0.87	1.77
Spline						
Year*vigour (D)	176.44 (1.00)**	32.29 (1.95)**	102.69 (1.00)**	81.66 (1.00)**	11.35 (2.35)**	43.89 (4.62)**
Year*vigour (ND)	16.64 (3.76)**	8.07 (1.00)**	27.49 (3.95)**	31.13 (2.37)**	7.29 (1.00)**	18.97 (4.60)**
Dbh	4.28 (1.00)*	2.41 (1.00)	29.32 (3.24)**	7.01 (1.00)**	8.17 (1.00)**	0.35 (1.00)
R^2	0.52	0.34	0.66	0.56	0.22	0.21

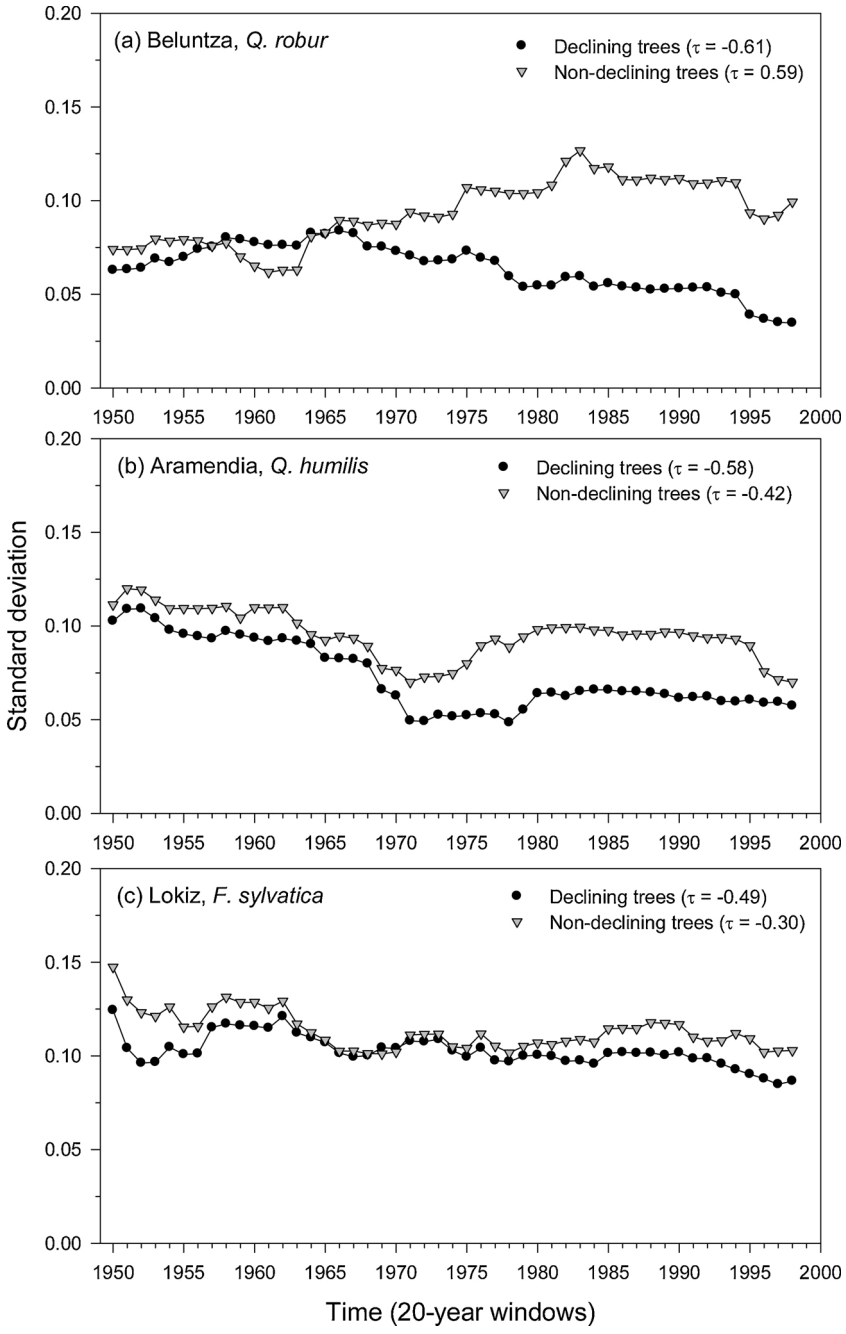

Fig. 2. The standard deviation of the mean growth series of declining and non-declining trees can be used as an early-warning signal of impending dieback. The trends of the standard deviation were assessed using the Kendall τ statistic.

3.4. Early-warning signals in growth series

The standard deviation of growth series showed a more pronounced long-term decrease in declining than in non-declining trees in one site of each species: Beluntza for *Q. robur*, Aramendia for *Q. humilis*, and Lokiz for *F. sylvatica* (Fig. 2). The trends of the standard deviation were negative in all these cases, excepting in non-declining *Q. robur* trees from the Beluntza site, and started diverging between the two vigour classes from the 1970s onwards. In the other three sites no clear differences in standard deviation between declining and non-declining trees were observed (Fig. S7).

3.5. Relationships between climate and growth

In the case of the Beluntza *Q. robur* site, growth of declining trees was negatively correlated with January mean minimum air temperature, precipitation and cloud cover (Table 4). This negative influence of January cold, wet and cloudy conditions on growth is interesting since January mean minimum air temperatures are significantly increasing since 1950 (Fig. S8). In contrast, high minimum air temperatures in July improved the growth of both declining and non-declining trees. In the Alsasua *Q. robur* site, growth of declining trees was constrained by warm and dry June conditions. In both *Q. robur* sites, warm September conditions improved growth. In the Galdeano *Q. humilis* site, wet and cloudy prior winter conditions and warm summers enhanced growth. In the Aramendia *Q. humilis* site, warm and wet springs and summer also reinforced growth. In the Eraso *F. sylvatica* site, warm, bright and dry summers (June, July) reduced growth, particularly in declining trees. Warm conditions in the prior autumn also were related to low growth rates. In the Lokiz site, warm and dry June conditions with low cloudiness were also responsible of growth decline in *F. sylvatica* trees. In July, high air temperatures also reduced growth, whereas cloudy conditions in July and August were related to growth improvement in declining trees. Growth increased with prior December foggy conditions in Beluntza (*Q. robur*) and Eraso (*F. sylvatica*), but decreased in response to prior November foggy conditions in Aramendia (*Q. humilis*) and Lokiz (*F. sylvatica*) (Table S2). May foggy conditions were also associated with decreased growth in Beluntza, whereas a foggy September improved growth in Eraso.

Moving correlations between selected climate variables and growth series showed that growth of declining trees is becoming increasingly limited by: higher minimum air temperatures in January in the Beluntza *Q. robur* site, low cloud cover amount in June in the Alsasua *Quercus robur* site, and less precipitation in July in the Aramendia *Q. humilis* site (Fig. 3). In the other moving correlations no significant differences between declining and non-declining trees were noted. Specifically, dry previous-November conditions decreased growth of *Q. humilis* in the Galdeano site, whereas the influence of summer precipitation on *F. sylvatica* growth is losing weight since the 2010s.

3.6. Relationships between drought and growth

The *F. sylvatica* declining trees showed the highest significant correlations with 1-month SPEI values (SPEI1) in April, May and June in both sites, and also for 3-month SPEI values (SPEI3) in July in the Lokiz site (Fig. S9). A similar signal with SPEI3 was observed in July for the declining *Q. humilis* trees from the Aramendia site, but also with SPEI1 in January in the case of non-declining trees. In contrast, *Q. humilis* growth and SPEI were not significantly correlated in Galdeano site. In the Alsasua *Q. robur* site, the main growth responses were observed in June and July for SPEI3 regardless the tree vigour, and in Beluntza they were found for SPEI1 in April.

3.7. Links between atmospheric patterns, climate and growth

Positive SOI values in the prior autumn and winter and in March were negatively correlated with *Q. robur* growth (Table 5). A similar signal was observed considering prior autumn and *F. sylvatica* in the Lokiz site. Positive NAO values in January were related to growth reductions of declining *Q. humilis* trees in Aramendia, but positive NAO values in March enhanced growth of non-declining *F. sylvatica* trees in Eraso. Positive WeMO values in the prior autumn and winter were associated with improved growth of declining trees in some sites (Bertiz, Aramendia, Eraso). In Eraso, spring and summer WeMO values were negatively correlated with growth. In Galdeano, growth of declining trees decreased in response to positive WeMO values in June, and this relationship has intensified after the dry mid 1990s (Fig. S10).

3.8. Water-use efficiency in declining and non-declining trees

The mean (± SE) values of wood $\delta^{13}C$ for 1968–2007 (5-ring pools) were -25.86 ± 0.09‰, -26.82 ± 0.10‰, and -26.56 ± 0.10‰ for *Q. robur*, *Q. humilis* and *F. sylvatica*, respectively. Considering the mean iWUE values of declining and non-declining trees, we found significant differences in *Q. robur* ($t = 2.59$, $p = 0.018$) and *F. sylvatica* ($t = 2.21$, $p = 0.047$) because declining trees showed higher iWUE (Fig. 4).

The means of $\delta^{13}C$ and derived iWUE individual values for the two most recent periods (2008–2012, 2013–2017) did not differ significantly between declining and non-declining trees in most cases (*Q. robur*, 2008–2012, $t = 1.72$, $p = 0.105$, 2013–2017, $t = 1.60$, $p = 0.129$, *Q. humilis*, 2008–2012, $t = 0.66$, $p = 0.516$, 2013–2017, $t = 0.03$, $p = 0.976$, *F. sylvatica*, 2008–2012, $t = 0.53$, $p = 0.610$). However, in the case of *F. sylvatica* and for 2013–2017, non-declining trees presented, on average, a 3.6 % higher iWUE than declining trees ($t = 2.88$, $p = 0.032$). Lastly, we found a significant correlation ($r = 0.79$, $p = 0.02$) of the differences in growth and iWUE between declining and non-declining in the *Q. humilis* Aramendia site (Fig. 5).

4. Discussion

We documented dieback episodes in response to climate extremes such as drought and cold spells (in the Beluntza *Q. robur* site) in several angiosperms from temperate forests located in northern Spain. European temperate forests dominated by oak and beech species have shown productivity losses, canopy dieback and mortality after past drought as has been widely documented in central Europe (Bréda et al., 2006). Regarding our hypotheses we found: (i) lower growth rates in more defoliated, declining trees but growth variability (standard deviation) was not always lower, (ii) more responsiveness to drought in declining trees in some (e.g., Aramendia *Q. humilis* site, Lokiz *F. sylvatica* site) but not all sites, and (iii) higher iWUE in *Q. robur* and *F. sylvatica* declining trees with a recent trend reversal in *F. sylvatica* since non-declining trees showed higher iWUE in the last 5-year period. Finally, no relationship was found when comparing differences in growth and iWUE between non-declining and declining trees, except in the case of *Q. humilis*.

We found the scenario characterized by lower growth and higher iWUE in declining *Q. robur* and *F. sylvatica* trees. This efficient water-use strategy could be caused by increased evapotranspiration rates and reduced g_s in *F. sylvatica* to sustain hydraulic functions but decreasing long-term carbon uptake (Gessler et al., 2007; Peiffer et al., 2014), whereas the risk of carbon starvation should be lower in the more anisohydric *Q. robur*. The recent reduction of iWUE in declining *F. sylvatica* trees would suggest a poor regulation of gas and water exchange through leaves leading to excessive water loss through leaves (Hentschel et al., 2016), but not necessarily to hydraulic impairment (Delaporte et al., 2016). Such inefficient response could characterize declining *F. sylvatica* trees prone to die, and indicates they are less responsive in terms of stomatal closure to dry-warm conditions (reduced soil water content, rising air temperatures and increasing vapor pressure deficit) as hypothesized by Michelot-Antalik et al. (2019). In declining *Quercus frainetto* trees, a lower iWUE related to increased water loss through transpiration was also observed (Colangelo et al., 2017a). A better

Table 4
Pearson correlations calculated between the mean series of ring-width indices of non-declining (ND) and declining (D) trees and monthly climate variables (Tx, mean maximum air temperatures, Tn, mean minimum air temperatures, Pr, precipitation, Cc, cloud cover). Correlations were calculated from the prior September (s) to the current September (S) considering the common 1950–2016 period. Only variables significant at the 0.05 level are presented (note that $r > |0.29|$ is significant at the 0.01 level).

Species	Site	Climate variable	Months																									
			s		o		n		d		J		F		M		A		M		J		J		A		S	
			ND	D	ND	D	ND	D	ND	D	ND	D	ND	D	ND	D	ND	D	ND	D	ND	D	ND	D	ND	D	ND	D
Q. robur	BE	Tx																										0.24
		Tn										−0.30											0.32	0.29				
		Pr									−0.24	−0.31																
		Cc										−0.24																
	AL	Tx																				−0.32					0.26	0.24
		Tn																							0.30			
		Pr																			0.25	0.26						
		Cc																				0.36						
Q. humilis	GA	Tx																0.25					0.22					
		Tn																				0.24						
		Pr	0.26					0.31	0.29																			
		Cc							0.28						−0.24													
	AR	Tx		−0.26				0.29																				
		Tn	0.24														0.30											
		Pr																		0.24				0.37				
		Cc																		0.29								
F. sylvatica	ER	Tx			−0.29		−0.25														−0.35	−0.32		−0.28				
		Tn			−0.26																−0.32	−0.29						
		Pr																	0.26			0.29			0.33			
		Cc																					0.25	0.29		0.26		
	LO	Tx																			−0.25	−0.39	−0.27	−0.39				
		Tn															0.25					−0.25						
		Pr																			0.32	0.39						
		Cc																			0.28	0.43		0.32		0.27		

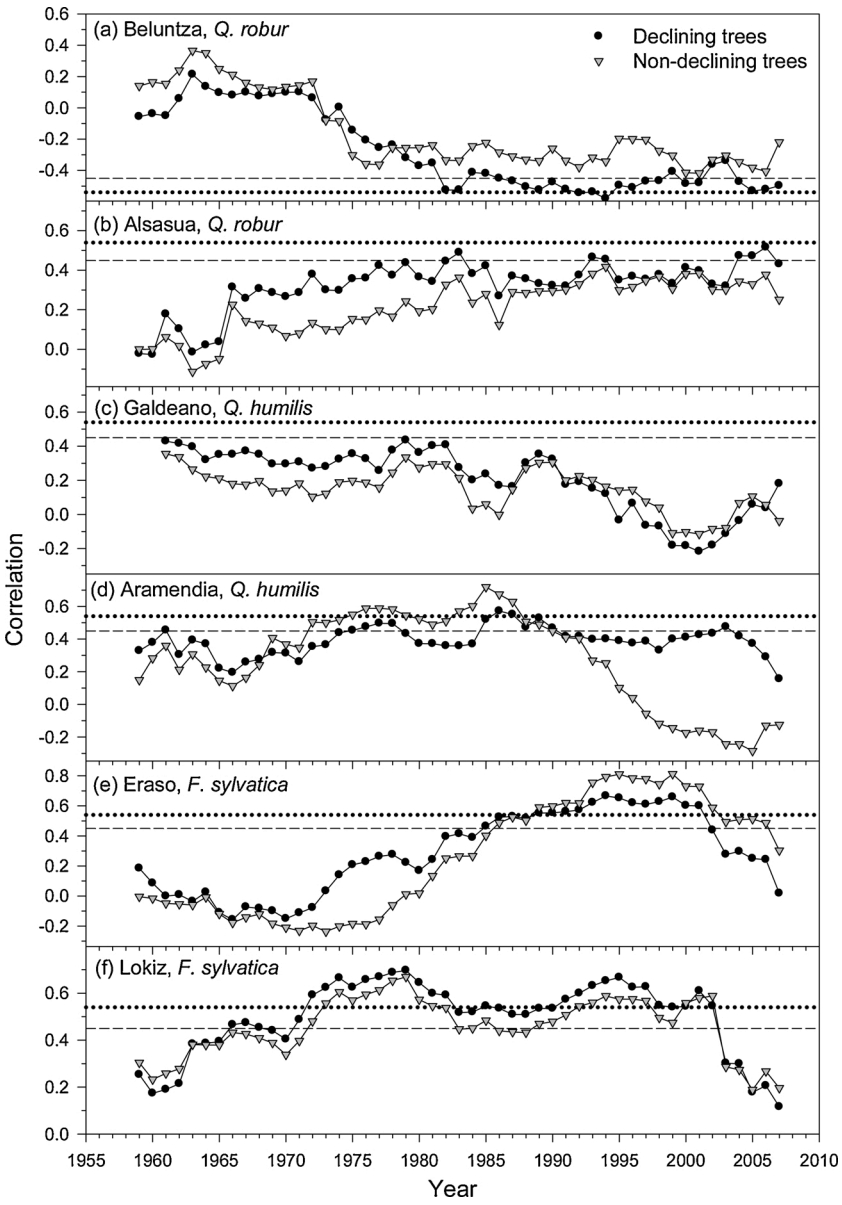

Fig. 3. Moving correlations calculated between several climate variables and mean series of ring-width indices of declining (black symbols) and non-declining (grey symbols) trees considering 20-year long intervals: (a) mean minimum air temperature in January, Beluntza *Quercus robur* site, (b) cloud cover in June, Alsasua *Quercus robur* site, (c) previous precipitation in November, Galdeano *Quercus humilis* site, (d) precipitation in July, Aramendia *Quercus humilis* site, (e) precipitation in June, Eraso *Fagus sylvatica* site, and (f) precipitation in July, Lokiz *Fagus sylvatica* site. The horizontal dashed and dotted lines indicate the 0.05 and 0.01 significance levels, respectively.

interpretation of our findings would benefit from using ^{18}O wood data to disentangle if increases in iWUE are due to either high photosynthetic rate, as proposed by Gessler et al. (2018), vs. low stomatal conductance rate (e.g., Granda et al., 2017).

In species dominant in mesic sites such as *Q. robur*, growth decline, dieback and rising mortality rates have been attributed to multiple stress factors differently affecting declining and non-declining trees as winter frosts, spring droughts and pests (Losseau et al., 2020). In this species, warm-dry conditions during the previous autumn and current spring and summer have been associated with reduced radial growth (Rozas, 2002; Lebourgeois et al., 2004; Matisons et al., 2012). Some studies have revealed that dieback is a long-term process related to past droughts with declining *Q. robur* trees showing growth depression about 20 years before tree death (Drobyshev et al., 2007, 2008, Andersson et al., 2011). Here we showed that the divergence in growth between declining and non-declining *Q. robur* trees went back at least 15–30 years before the dieback onset. However, differences in growth between both vigour types were observed even since the 1950s indicating that declining trees were predisposed to show dieback due to their consistently lower growth rates. In addition, climate extremes as the 1971 cold spell amplified the growth divergence and could have also predisposed to dieback.

Warmer winter to early-spring conditions could partially explain the growth decline in the wet Beluntza *Q. robur* site, but the role played by winter cold spells is unknown or could be indirectly linked to soil waterlogging. In ring-porous, deciduous oaks from temperate and continental sites, earlywood vessel lumen area decreased in response to warm or dry late-winter to early-spring conditions (García-González and Eckstein, 2003; Tardif and Conciatori, 2006; Fonti et al., 2009; Alla and Camarero, 2012). This can be explained because in these species earlywood formation is very dependent on stored reserves (Vincent-Barbaroux et al., 2019), and warmer winters could increase respiration and carbohydrate consumption reducing spring growth. In contrast, *Q. robur* growth was reduced by low winter soil temperatures near the northernmost limit of distribution of the species (Helama et al., 2016). In these northern stands, growth reduction was attributed to winter cold spells which negatively affected insufficiently hardened trees regardless their vigour status (Matisons et al., 2013).

The low growth sensitivity of *Q. robur* to drought in the study sites is expected since they were characterized by wet soils with poor drainage.

Table 5
Pearson correlations calculated between the mean series of ring-width indices of non-declining (ND) and declining (D) trees and monthly values of three climate indices (NAO, North Atlantic Oscillation, SOI, Southern Oscillation Index, WeMO, Western Mediterranean Oscillation). Correlations were calculated from the prior September (s) to the current September (S) considering the common 1950–2016 period. Only variables significant at the 0.05 level are presented ($r > |0.29|$ is significant at the 0.01 level).

Species	Site	Climate index	Months																			
			s		o		n		d		J		F		M		A		J		A		S	
			ND	D	ND	D	ND	D	ND	D	ND	D	ND	D	ND	D	ND	D	ND	D	ND	D	ND	D
Q. robur	BE	NAO																						
		SOI	−0.37	−0.30	−0.41	−0.32	−0.32	−0.31			−0.31	−0.26												
		WeMO		0.25						0.26														
	AL	NAO																						
		SOI	−0.32	−0.36	−0.39	−0.34	−0.33	−0.36	−0.28	−0.33	−0.28	−0.32		−0.25	−0.32		−0.35							
		WeMO																						
		NAO																						
	GA	SOI			−0.28										−0.26				−0.33			−0.27		
		WeMO																		−0.40				
Q. humilis		NAO										−0.26												
	AR	SOI																						
		WeMO				0.24																−0.26		
		NAO													0.31									
	ER	SOI		−0.25											−0.24		−0.28			−0.35			−0.31	
		WeMO		0.28														0.24		0.24			−0.24	−0.36
F. sylvatica		NAO																						
	LO	SOI	−0.28	−0.32	−0.24											−0.25								
		WeMO																				0.25		

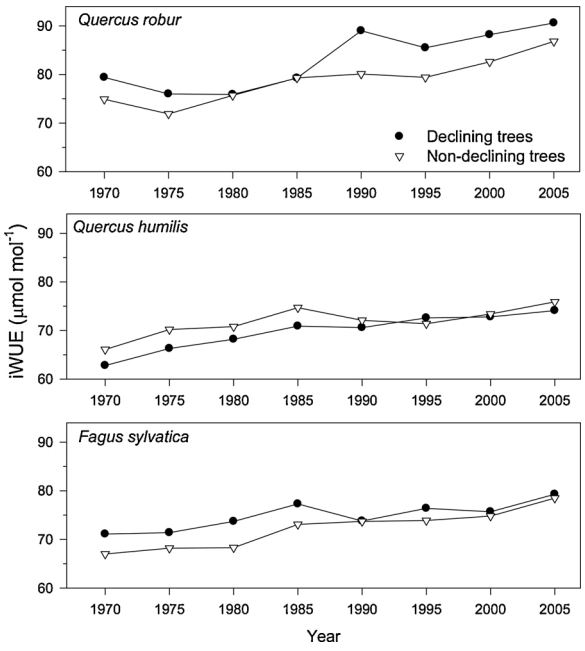

Fig. 4. Intrinsic water-use efficiency (iWUE) inferred from $\delta^{13}C$ in 5-ring wood samples of declining (filled symbols) and non-declining (empty symbols) trees. The eight 5-year periods considered were: 1968–1972, 1973–1977, 1978–1982, 1983–1987, 1988–1992, 1993–1997, 1998–2002, and 2003–2007.

In fact, increasingly wetter conditions after the 1980s linked to shifts in the ENSO caused dieback of *Q. robur* stands in NW Spain due to soil water logging (Rozas and García-González, 2012). We also detected associations between *Q. robur* growth and the winter-spring ENSO confirming the importance of these seasons for this species and pointing to indirect relationships with summer cloudiness and foggy days (Rozas et al., 2015). In Beluntza a prior foggy December increased growth which can correspond to stable pressures and a better drainage of its soils. However, a foggy late spring can reduce air temperatures and growth rates, whilst a foggy early autumn could alleviate water shortage as observed in the Eraso *F. sylvatica* site.

In the case of *Q. humilis*, the higher responsiveness to summer water shortage of declining trees in the Aramendia site indicates a dominant role played by drought stress as dieback cause. The growth decline was triggered by successive droughts and has occurred as summer conditions became increasingly warmer and less cloudy. Tree size was also relevant explaining dieback in this and other sites, and this agrees with previous observation showing that declining trees tend to be smaller, in terms of diameter and height, than coexisting, non-declining trees (Colangelo et al., 2017b). In southern Europe, dieback of oak species functionally similar to *Q. humilis* has been often attributed to drought stress, often in sites with shallow soils showing low water holding capacity (Amorini et al., 1996; Di Filippo et al., 2010; Camarero et al., 2015, 2016, Colangelo et al., 2017a). The growth- iWUE coupling between declining and non-declining trees was only observed in the Aramendia *Q. humilis* site, providing partial support to Gessler et al. (2018) hypothesis that declining trees will feature low growth rates and be less water-use efficient. Finally, in the Galdeano *Q. humilis* site, we also detected a signal of the WeMO in the growth of declining trees indicating a higher vulnerability to drought stress which was contingent on site conditions. Unexpectedly, we found no associations between the NAO and tree growth despite positive NAO phases correspond to warm-dry winter and spring conditions and reduced tree growth in northern Spain (Camarero, 2011) and Italy (Piovesan and Schirone, 2000). This unexpected NAO-dissociation may be caused by a low coupling of local climate conditions to regional climate patterns due to topographical effects (e.g., slope, aspect).

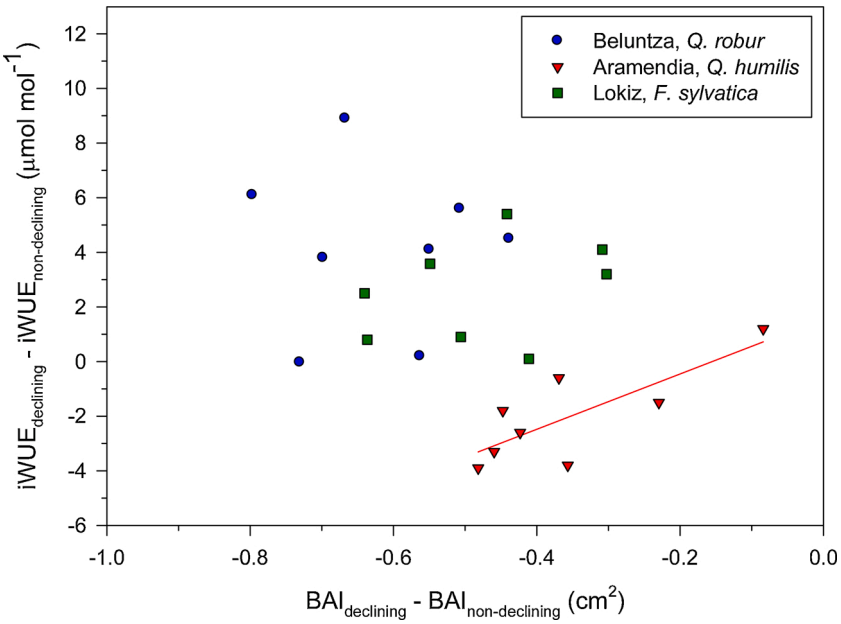

Fig. 5. Differences in growth and intrinsic water-use efficiency (iWUE) between declining and non-declining trees calculated for 5-year periods. The line indicates the significant relationship in the case of *Q. humilis*.

Lower post-drought growth rates and poor crown conditions (leaf shedding, death of shoots and buds) characterize forest dieback and may indicate impending tree death (Cailleret et al., 2017). For instance, in *F. sylvatica*, when the proportion of canopy dieback surpassed the 58 % threshold tree death was unavoidable (Chakraborty et al., 2017). We found that *F. sylvatica* growth was reduced by warm-dry summer conditions with clear skies which explains why late-summer foggy days could alleviate drought stress in the Eraso site. The effect of drought on growth occurred regardless the divergence between declining and non-declining trees, which was short (5–10 years) and significant in one site (Eraso). The sensitivity to drought in this species agrees with its moderately anisohydric behaviour and may explain the reversal in iWUE trends of declining trees in Lokiz, which showed a loss of water-use efficiency close to the dieback onset suggesting a loss of control of stomatal closure (Aranda et al., 2000; Michelot-Antalik et al., 2019). The increasing relevance of summer drought and reduced soil water availability as constraints of *F. sylvatica* growth has been shown in the core of its distribution range across central Europe (Dittmar et al., 2003; Lebourgeois et al., 2005; Michelot et al., 2012; Zang et al., 2014; Dulamsuren et al., 2017; Harvey et al., 2020; Hacket-Pain et al., 2017), but also in its rear edge across southern Europe (Jump et al., 2006; Di Filippo et al., 2007; Piovesan et al., 2008; Serra-Maluquer et al., 2019).

Here we show that more attention should be paid to other regional climate factors such as cloud cover or fog which could reverse or alter the species sensitivity to summer drought (Rozas et al., 2015), and atmospheric patterns as the WeMO which influence summer precipitation. Climate warming could also induce and earlier leaf unfolding in *F. sylvatica* (Čufar et al., 2008), and make some early-bursting trees prone to late frost damage (Gazol et al., 2019). In addition, local factors should be considered such as soil water availability which can affect nutrient uptake (Gessler et al., 2007, 2016, Delaporte et al., 2017) and fine root mortality (Meier and Leuschner, 2008). Tree size and neighbourhood interactions, often related to management legacies, are also relevant drivers of growth sensitivity to drought in *F. sylvatica* (Gazol et al., 2018a; Laskurain et al., 2018; Mausolf et al., 2018).

The smaller size observed in declining beech and oak trees could reflect: (i) the formation of less intensive root systems making them less able to access soil water pools during the dry summer (Ripullone et al., 2020), or (ii) a lower growth recovery capacity. Further research should consider the effects of successive droughts on growth and functioning of adult trees which could adapt by readjusting carbon allocation. In experiments based on saplings, repeated droughts induced high xylem embolism levels (Tomasella et al., 2019) and carbon starvation (Chuste et al., 2020). Deciduous oak and beech species from temperate forests show more rapid post-drought recovery and higher resistance than evergreen pines from dry sites (Anderegg et al., 2015; Gazol et al., 2018b). But we do not know if this resistance also entails carry-over effects after successive droughts impairing the hydraulic functioning and carbon pools of declining trees. A limited resistance of declining trees and a higher impact of drought on growth could explain dieback and selective mortality in temperate forests (DeSoto et al., 2020). To test if the selective thinning of stands showing abundant declining and dying trees improves their long-term vitality visual assessments of defoliation could be complemented with long-term growth records based on tree-ring analyses.

5. Conclusions

In three species dominant in temperate forests, declining trees showed smaller size in most sites and lower growth rates in all sites. Declining trees tended to show lower growth variability, but not in all sites. The growth divergence between declining and non-declining trees was significant and long in *Q. robur* (15–30 years) and short in the Eraso *F. sylvatica* site (5–10 years). Dieback was triggered by drought, but in wet sites (Beluntza *Q. robur* site) cold spells and waterlogged soils contributed to the growth decline. The species most responsive to summer drought was *F. sylvatica*. In *Q. humilis*, growth and iWUE differences between declining and non-declining trees were coupled. In *F. sylvatica*, declining trees showed a recent reversal in iWUE and became less water-use efficient close to the dieback onset.

Declaration of Competing Interest

The authors declare that they have no known competing financial interests or personal relationships that could have appeared to influence the work reported in this paper.

Acknowledgments

We thank the support of Beluntza, Estella and Alsasua forest guards

offices (Basque and Navarra Governments) and, particularly, the interest and guidance of J.M. Vadillo (Navarra Govt.) and Alejandro Cantero (Neiker, Basque Govt.). This study was supported by projects FunDiver (CGL2015-69186-C2-1-R) and FORMAL (RTI2018-096884-B-C31) from the Spanish Ministry of Science and Innovation, Innovation and Universities. C. A-M. was supported by Ramon y Cajal fellowship (RYC-2017-22830). We acknowledge the E-OBS dataset from the EU-FP6 project UERRA (http://www.uerra.eu) and the Copernicus Climate Change Service, and the data providers in the ECAandD project (https://www.ecad.eu).

Appendix A. Supplementary data

Supplementary material related to this article can be found, in the online version, at doi:https://doi.org/10.1016/j.dendro.2021.125812.

References

Adams, H.D., Zeppel, M.J.B., Anderegg, W.R.L., Hartmann, H., Landhäusser, S.M., et al., 2017. A multi-species synthesis of physiological mechanisms in drought-induced tree mortality. Nat. Ecol. Evol. 1, 1285–1291.

Akaike, H., 1974. A new look at the statistical model identification. Automatic control. IEEE Trans. Automatic Control 19, 716–723.

Alla, A.Q., Camarero, J.J., 2012. Contrasting responses of radial growth and wood anatomy to climate in a Mediterranean ring-porous oak: implications for its future persistence or why the variance matters more than the mean. Eur. J. For. Res. 131, 1537–1550.

Allen, C.D., Breshears, D.D., McDowell, N.G., 2015. On underestimation of global vulnerability to tree mortality and forest die-off from hotter drought in the Anthropocene. Ecosphere 6, 1–55.

Amorini, E., Biocca, M., Manetti, M.C., Motta, E., 1996. A dendroecological study in a declining oak coppice stand. Ann. For. Sci. 53, 731–742.

Anderegg, W.R.L., Schwalm, C., Biondi, F., Camarero, J.J., Koch, G., et al., 2015. Pervasive drought legacies in forest ecosystems and their implications for carbon cycle models. Science 349, 528–532.

Andersson, A., Milberg, P., Bergman, K.-O., 2011. Low pre-death growth rates of oak (*Quercus robur* L.) –Is oak death a long-term process induced by dry years? Ann. For. Sci. 68, 159–168.

Aranda, I., Gil, L., Pardos, J.A., 2000. Water relations and gas exchange in Fagus sylvatica L. and *Quercus petraea* (Mattuschka) Liebl. in a mixed stand at their southern limit of distribution in Europe. Trees 14, 344–352.

Babst, F., Bouriaud, O., Poulter, B., Trouet, V., Girardin, M.P., Frank, D.C., 2019. Twentieth century redistribution in climatic drivers of global tree growth. Sci. Adv. 5 eaat4313.

Bréda, N., Huc, R., Granier, A., Dreyer, E., 2006. Temperate forest trees and stands under severe drought: a review of ecophysiological responses, adaptation processes and long-term consequences. Ann. For. Sci. 63, 625–644.

Cailleret, M., Jansen, S., Robert, E.M.R., Desoto, L., Aakala, T., et al., 2017. A synthesis of radial growth patterns preceding tree mortality. Glob. Change Biol. 23, 1675–1690.

Camarero, J.J., 2011. Direct and indirect effects of the North Atlantic oscillation on tree growth and forest decline in northeastern Spain. In: Vicente-Serrano, S.M., Trigo, R. M. (Eds.), Hydrological, Socioeconomic and Ecological Impacts of the North Atlantic Oscillation in the Mediterranean Region. Springer, Heidelberg, pp. 129–152.

Camarero, J.J., Fajardo, A., 2017. Poor acclimation to current drier climate of the long-lived tree species Fitzroya cupressoides in the temperate rainforest of southern Chile. Agric. For. Meteorol. 239, 141–150.

Camarero, J.J., Gazol, A., Sangüesa-Barreda, G., Oliva, J., Vicente-Serrano, S.M., 2015. To die or not to die: early-warning signals of dieback in response to a severe drought. J. Ecol. 103, 44–57.

Camarero, J.J., Sangüesa-Barreda, G., Vergarechea, M., 2016. Prior height, growth, and wood anatomy differently predispose to drought-induced dieback in two Mediterranean oak species. Ann. For. Sci. 73, 341–351.

Cavin, L., Mountford, E.P., Peterken, G.F., Jump, A.S., 2013. Extreme drought alters competitive dominance within and between tree species in a mixed forest stand. Funct. Ecol. 27, 1424–1435.

Chakraborty, T., Saha, S., Matzarakis, A., Reif, A., 2017. Influence of multiple biotic and abiotic factors on the crown die-back of European beech trees at their drought limit. Flora 229, 58–70.

Chuste, P., Maillard, P., Bréda, N., Levillain, J., Thirion, E., et al., 2020. Sacrificing growth and maintaining a dynamic carbohydrate storage are key processes for promoting beech survival under prolonged drought conditions. Trees 34, 381–394.

Colangelo, M., Camarero, J.J., Battipaglia, G., Borghetti, M., De Micco, V., et al., 2017a. A multi-proxy assessment of dieback causes in a Mediterranean oak species. Tree Physiol. 37, 617–631.

Colangelo, M., Camarero, J.J., Borghetti, M., Gazol, A., Ripullone, F., 2017b. Size matters a lot: drought-affected Italian oaks are smaller and show lower growth prior to tree death. Front. Plant Sci. 8, 135.

Cook, E.R., Krusic, P., 2005. A Tree-ring Standardization Program Based on Detrending and Autoregressive Time Series Modeling, with Interactive Graphics. Tree-Ring Laboratory, Lamont Doherty Earth Observatory. Columbia Univ., New York.

Cornes, R., van der Schrier, G., van den Besselaar, E.J.M., Jones, P.D., 2018. An ensemble version of the E-OBS temperature and precipitation datasets. J. Geophys. Res.-Atmosph. 123, 9391–9409.

Čufar, K., Prislan, P., de Luis, M., Gričar, J., 2008. Tree-ring variation, wood formation and phenology of beech (*Fagus sylvatica*) from a representative site in Slovenia, SE Central Europe. Trees 22, 749–758.

D'Orangeville, L., Maxwell, J., Kneeshaw, D., Pederson, N., Duchesne, L., et al., 2018. Drought timing and local climate determine the sensitivity of eastern temperate forests to drought. Glob. Change Biol. 24, 2339–2351.

Dakos, V., Carpenter, S.R., Brock, W.A., Ellison, A.M., Guttal, V., et al., 2012. Methods for detecting early warnings of critical transitions in time series illustrated using simulated ecological data. PLoS One 7, e41010.

Damesin, C., Rambal, S., 1995. Field study of leaf photosynthetic performance by a Mediterranean deciduous oak tree (*Quercus pubescens*) during a severe summer drought. New Phytol. 131, 159–167.

Delaporte, A., Bazot, S., Damesin, C., 2016. Reduced stem growth, but no reserve depletion or hydraulic impairment in beech suffering from long-term decline. Trees 30, 265–279.

Delaporte, A., Zanella, A., Vincent, G., Bugeat, M., Damesin, C., Bazot, S., 2017. Structural and functional differences in the belowground compartment of healthy and declining beech trees. Appl. Soil Ecol. 117–118, 106–116.

DeSoto, L., Cailleret, M., Sterck, F., Jansen, S., Kramer, K., et al., 2020. Low growth resilience to drought is related to future mortality risk in trees. Nat. Comm. 11, 545.

Di Filippo, A., Biondi, F., Čufar, K., De Luis, M., Grabner, M., et al., 2007. Bioclimatology of beech (*Fagus sylvatica* L.) in the Eastern Alps: spatial and altitudinal climatic signals identified through a tree-ring network. J. Biogeogr. 34, 1873–1892.

Di Filippo, A., Alessandrini, A., Biondi, F., Blasi, S., Portoghesi, L., Piovesan, G., 2010. Climate change and oak growth decline: dendroecology and stand productivity of a Turkey oak (*Quercus cerris* L.) old stored coppice in Central Italy. Ann. For. Sci. 67, 706.

Dittmar, C., Zech, W., Elling, W., 2003. Growth variations of Common beech (*Fagus sylvatica* L.) under different climatic and environmental conditions in Europe – a dendroecological study. For. Ecol. Manage. 173, 63–78.

Dobbertin, M., 2005. Tree growth as indicator of tree vitality and of tree reaction to environmental stress: a review. Eur. J. For. Res. 124, 319–333.

Drobyshev, I., Linderson, H., Sonesson, K., 2007. Temporal mortality pattern of pedunculate oaks in southern Sweden. Dendrochronologia 24, 97–108.

Drobyshev, I., Niklasson, M., Eggertsson, O., Linderson, H., Sonesson, K., 2008. Influence of annual weather on growth of pedunculate oak in southern Sweden. Ann. For. Sci. 65, 512.

Druckenbrod, D.L., Martin-Benito, D., Orwig, D.A., et al., 2019. Redefining temperate forest responses to climate and disturbance in the eastern United States: new insights at the mesoscale. Glob. Ecol. Biogeogr. 28, 557–575.

Dulamsuren, C., Hauck, M., Kopp, G., Ruff, M., Leuschner, C., 2017. European beech responds to climate change with growth decline at lower, and growth increase at higher elevations in the center of its distribution range (SW Germany). Trees 31, 673–686.

Farquhar, G.D., O' Leary, M.H., Berry, J.A., 1982. On the relationship between carbon isotope discrimination and the inter-cellular carbon-dioxide concentration in leaves. Austral. J. Plant Physiol. 9, 121–137.

Farquhar, G.D., Ehleringer, J.R., Hubick, K.T., 1989. Carbon isotope discrimination and photosynthesis. Ann. Rev. Plant Physiol. Plant Molec. Biol. 40, 503–537.

Filewod, B., Thomas, S.C., 2014. Impacts of a spring heat wave on canopy processes in a northern hardwood forest. Glob. Change Biol. 20, 360–371.

Fonti, P., Treydte, K., Osenstetter, S., Frank, D., Esper, J., 2009. Frequency-dependent signals in multi-centennial oak vessel data. Palaeogeogr. Palaeoclimatol. Palaeoecol. 275, 92–99.

Frelich, L.E., Montgomery, R.A., Oleksyn, J., 2015. Northern temperate forests. In: Peh, K.S.H., Corlett, R.T., Bergeron, Y. (Eds.), Routledge Handbook of Forest Ecology. Routledge, London.

Fritts, H.C., 1962. The relation of growth ring widths in American beech and white oak to variations in climate. Tree-Ring Bull. 25, 2–10.

García-González, I., Eckstein, D., 2003. Climatic signal of earlywood vessels of oak on a maritime site. Tree Physiol. 23, 497–504.

Gazol, A., Camarero, J.J., Anderegg, W.R.L., Vicente-Serrano, S.M., 2017. Impacts of droughts on the growth resilience of Northern Hemisphere forests. Glob. Ecol. Biogeogr. 26, 166–176.

Gazol, A., Camarero, J.J., Jiménez, J.J., Moret-Fernández, D., López, M.V., et al., 2018a. Beneath the canopy: linking drought-induced forest die off and changes in soil properties. For. Ecol. Manage. 422, 294–302.

Gazol, A., Camarero, J.J., Vicente-Serrano, S.M., Sánchez-Salguero, R., Gutiérrez, E., et al., 2018b. Forest resilience to drought varies across biomes. Global Change Biol. 24, 2143–2158.

Gazol, A., Camarero, J.J., Colangelo, M., De Luis, M., Martínez del Castillo, E., Serra-Maluquer, X., 2019. Summer drought and spring frost, but not their interaction, constrain European beech and Silver fir growth in their southern distribution limits. Agric. For. Meteorol. 278, 107695.

Gessler, A., Keitel, C., Kreuzwieser, J., Matyssek, R., Seiler, W., Rennenberg, H., 2007. Potential risks for European beech (*Fagus sylvatica* L.) in a changing climate. Trees 21, 1–11.

Gessler, A., Schaub, M., McDowell, N.G., 2016. The role of nutrients in drought-induced tree mortality and recovery. New Phytol. 214, 513–520.

Gessler, A., Cailleret, M., Joseph, J., Schönbeck, L., Schaub, M., et al., 2018. Drought induced tree mortality – a tree-ring isotope based conceptual model to assess mechanisms and predispositions. New Phytol. 219, 485–490.

Giorgi, F., Lionello, P., 2008. Climate change projections for the Mediterranean region. Glob. Planet. Ch. 63, 90–104.
Granda, E., Alla, A.Q., Laskurain, N.A., Loidi, J., Sánchez-Lorenzo, A., Camarero, J.J., 2017. Coexisting oak species, including rear-edge populations, buffer climate stress through xylem adjustments. Tree Physiol. 38, 159–172.
Hacket-Pain, A.J., Lageard, J.G.A., Thomas, P.A., 2017. Drought and reproductive effort interact to control growth of a temperate broadleaved tree species (*Fagus sylvatica*). Tree Physiol. 37, 744–754.
Harris, I., Jones, P.D., Osborn, T.J., Lister, D.H., 2014. Updated high-resolution grids of monthly climatic observations –the CRU TS3.10 Dataset. Int. J. Climatol. 34, 623–642.
Harvey, J.E., Smiljanić, M., Scharnweber, T., Buras, A., Cedro, A., et al., 2020. Tree growth influenced by warming winter climate and summer moisture availability in northern temperate forests. Glob. Change Biol. 26, 2505–2518.
Helama, S., Sohar, K., Läänelaid, A., Mäkelä, H.M., Raisio, J., 2016. Oak decline as illustrated through plant–climate interactions near the northern edge of species range. Bot. Rev. 82, 1–23.
Hentschel, R., Hommel, R., Poschenrieder, W., Grote, R., Holst, J., et al., 2016. Stomatal conductance and intrinsic water use efficiency in the drought year 2003: a case study of European beech. Trees 30, 153–174.
Holmes, R.L., 1983. Computer-assisted quality control in tree–ring dating and measurement. Tree-Ring Bull. 43, 69–78.
Jump, A.S., Hunt, J.M., Peñuelas, J., 2006. Rapid climate change-related growth decline at the southern range edge of *Fagus sylvatica*. Glob. Change Biol. 12, 2163–2174.
Laskurain, N.A., Aldezabal, A., Odriozola, I., Camarero, J.J., Olano, J.M., 2018. The role of tree context: variation in the individual growth response to climate among neighbourhoods and species in a secondary forest. Forests 9, 43.
Lebourgeois, F., Cousseau, G., Ducos, Y., 2004. Climate-tree-growth relationships of *Quercus petraea* Mill. Stand in the Forest of Bercé ("Futaie des Clos", Sarthe, France). Ann. For. Sci. 61, 361–372.
Lebourgeois, F., Bréda, N., Ulrich, E., Granier, A., 2005. Climate-tree-growth relationships of European beech (*Fagus sylvatica* L.) in the French permanent plot network (RENECOFOR). Trees 19, 385–401.
Losseau, J., Jonard, M., Vincke, C., 2020. Pedunculate oak decline in southern Belgium: a long-term process highlighting the complex interplay among drought, winter frost, biotic attacks, and masting. Can. J. For. Res. 50, 380–389.
Manion, P.D., 1981. Tree Disease Concepts. Englewood Cliffs, Prentice Hall.
Martín-Vide, J., López-Bustins, J.A., 2006. The western mediterranean oscillation and rainfall in the Iberian Peninsula. Int. J. Climatol. 26, 1455–1475.
Matisons, R., Elferts, D., Brūmelis, G., 2012. Changes in climatic signals of English oak tree-ring width and crosssection area of earlywood vessels in Latvia during the period 1900–2009. For. Ecol. Manage. 279, 34–44.
Matisons, R., Elferts, D., Brūmelis, G., 2013. Possible signs of growth decline of pedunculate oak in Latvia during 1980–2009 in tree ring width and vessel size. Baltic For. 19, 137–142.
Mausolf, K., Wilm, P., Härdtle, W., Jansen, K., Schuldt, B., et al., 2018. Higher drought sensitivity of radial growth of European beech in managed than in unmanaged forests. Sci. Tot. Env. 642, 1201–1208.
Meier, I.C., Leuschner, C., 2008. Belowground drought response of European beech: fine root biomass and carbon partitioning in 14 mature stands across a precipitation gradient. Glob. Change Biol. 14, 2081–2095.
Michelot, A., Bréda, N., Damesin, C., Dufrêne, E., 2012. Differing growth responses to climatic variations and soil water deficits of *Fagus sylvatica, Quercus petraea* and *Pinus sylvestris* in a temperate forest. For. Ecol. Manage. 265, 161–171.
Michelot-Antalik, A., Granda, E., Fresneau, C., Damesin, C., 2019. Evidence of a seasonal trade-off between growth and starch storage in declining beeches: assessment through stem radial increment, non-structural carbohydrates and intra-ring $\delta^{13}C$. Tree Physiol. 39, 831–844.
Moreno, A., Hasenauer, H., 2015. Spatial downscaling of European climate data. Int. J. Climatol. 36, 1444–1458.
Pasho, E., Camarero, J.J., de Luis, M., Vicente-Serrano, S.M., 2011. Impacts of drought at different time scales on forest growth across a wide climatic gradient in north-eastern Spain. Agric. For. Meteorol. 151, 1800–1811.
Pedersen, B.S., 1998. The role of stress in the mortality of midwestern oaks as indicated by growth prior to death. Ecology 79, 79–93.
Pederson, N., Dyer, J.M., McEwan, R.W., Hessl, A.E., Mock, C.J., 2014. The legacy of episodic climatic events in shaping temperate, broadleaf forests. Ecol. Monogr. 84, 599–620.
Peiffer, M., Bréda, N., Badeau, V., Granier, A., 2014. Disturbances in European beech water relation during an extreme drought. Ann. For. Sci. 71, 821–829.
Pflug, E.E., Buchmann, N., Siegwolf, R., Schaub, M., Rigling, A., Arend, M., 2018. Resilient leaf physiological response of European beech (*Fagus sylvatica* L.) to summer drought and drought release. Front. Plant Sci. 9, 187.
Piovesan, G., Schirone, B., 2000. Winter North Atlantic oscillation effects on the tree rings of the Italian beech (*Fagus sylvatica* L.). Int. J. Biometeorol. 44, 121–127.
Piovesan, G., Biondi, F., Di Filippo, A., Alessandrini, A., Maugeri, M., 2008. Drought-driven growth reduction in old beech (*Fagus sylvatica* L.) forests of the central Apennines, Italy. Glob. Change Biol. 14, 1265–1281.
Pretzsch, H., Schütze, G., Uhl, E., 2013. Resistance of European tree species to drought stress in mixed versus pure forests: evidence of stress release by inter-specific facilitation. Plant Biol. 15, 483–495.
R Development Core Team, 2019. R: a Language and Environment for Statistical Computing. R Foundation for Statistical Computing, Vienna http:www.r-project.org.
Ripullone, F., Camarero, J.J., Colangelo, M., Voltas, J., 2020. Variation in the access to deep soil water pools explains tree-to-tree differences in drought-triggered dieback of Mediterranean oaks. Tree Physiol. 40, 591–604.
Rodó, X., Baert, E., Comin, F.A., 1997. Variations in seasonal rainfall in Southern Europe during the present century: relationships with the North Atlantic Oscillation and the El Niño-Southern Oscillation. Clim. Dyn. 13, 275–284.
Rozas, V., 2002. Detecting the impact of climate and disturbances on tree-rings of *Fagus sylvatica* L. and *Quercus robur* L. in a lowland forest in Cantabria, Northern Spain. Ann. For. Sci. 58, 237–251.
Rozas, V., García-González, I., 2012. Too wet for oaks? Inter-tree competition and recent persistent wetness predispose oaks to rainfall-induced dieback in Atlantic rainy forest. Glob. Planet. Ch. 94–95, 62–71.
Rozas, V., Camarero, J.J., Sangüesa-Barreda, G., Souto, M., García-González, I., 2015. Summer drought and ENSO-related cloudiness distinctly drive *Fagus sylvatica* growth near the species rear-edge in northern Spain. Agric. For. Meteorol. 201, 153–164.
Rubio-Cuadrado, A., Camarero, J.J., del Río, M., Sánchez-González, M., Ruiz-Peinado, R., et al., 2018. Long-term impacts of drought on growth and forest dynamics in a temperate beech-oak-birch forest. Agric. For. Meteorol. 259, 48–59.
Sánchez-Salguero, R., Camarero, J.J., Gutiérrez, E., González Rouco, F., Gazol, A., et al., 2017. Assessing forest vulnerability to climate warming using a process-based model of tree growth: bad prospects for rear-edges. Glob. Change Biol. 23, 2705–2719.
Serra-Maluquer, X., Gazol, A., Sangüesa-Barreda, G., Sánchez-Salguero, R., Rozas, V., Colangelo, M., Gutiérrez, E., Camarero, J.J., 2019. Geographically structured growth decline of rear-edge Iberian *Fagus sylvatica* forests after the 1980s shift toward a warmer climate. Ecosystems 22, 1325–1337.
Tardif, J.C., Conciatori, F., 2006. Influence of climate on tree rings and vessel features in red oak and white oak growing near their northern distribution limit, southwestern Quebec. Canada. Can. J. For. Res. 36, 2317–2330.
Tomasella, M., Nardini, A., Hesse, B.D., Machlet, A., Matyssek, R., Häberle, K.-H., 2019. Close to the edge: effects of repeated severe drought on stem hydraulics and non-structural carbohydrates in European beech saplings. Tree Physiol. 39, 717–728.
Vicente-Serrano, S.M., Beguería, S., López-Moreno, J.I., 2010. A multiscalar drought index sensitive to global warming: the stamdardized precipitation evapotranspiration index. J. Clim. 23, 1696–1718.
Vicente-Serrano, S.M., Tomas-Burguera, M., Beguería, S., Reig, F., Latorre, B., et al., 2017. A high-resolution dataset of drought indices for Spain. Data 2, 22.
Vincent-Barbaroux, C., Berveiller, D., Lelarge-Trouverie, C., Maia, R., Máguas, C., et al., 2019. Carbon-use strategies in stem radial growth of two oak species, one Temperate deciduous and one Mediterranean evergreen: what can be inferred from seasonal variations in the $\delta^{13}C$ of the current year ring? Tree Physiol. 39, 1329–1341.
Wood, S., 2006. Generalized Additive Models: an Introduction With R. Chapman and Hall/CRC Press, Boca Raton.
Wyckoff, P.H., Clark, J.D., 2002. The relationship between growth and mortality for seven co-occurring tree species in the southern Appalachian Mountains. J. Ecol. 90, 604–615.
Zang, C., Hartl-Meier, C., Dittmar, C., Rothe, A., Menzel, A., 2014. Patterns of drought tolerance in major European temperate forest trees: climatic drivers and levels of variability. Glob. Change Biol. 20, 3767–3779.